A Gaussian model for the membrane of red blood cells with cytoskeletal defects

Cyril Dubus, Jean-Baptiste Fournier

A Gaussian Model for the Membrane of Red Blood Cells with Cytoskeletal Defects

Cyril Dubus[1,2] and Jean-Baptiste Fournier[1,2,*]

[1] *Laboratoire Matière et Systèmes Complexes (MSC), UMR 7057 CNRS & Université Paris 7, 2 place Jussieu, F-75251 Paris Cedex 05, France*
[2] *Laboratoire de Physico-Chimie Théorique, UMR CNRS 7083 & ESPCI, 10 rue Vauquelin, F-75231 Paris Cedex 05, France*

(Dated: March 14, 2006)

We study a Gaussian model of the membrane of red blood cells: a "phantom" triangular network of springs attached at its vertices to a fluid bilayer with curvature elasticity and tension. We calculate its fluctuation spectrum and we discuss the different regimes and non-monotonic features, including the precise crossover at the mesh size between the already known limits with two different tensions and the renormalisation of the bending rigidity at low wavevectors. We also show that the non-diagonal correlations reveal, in "dark field", the cytoskeletal defects. As a first step toward a non-invasive defect spectroscopy, the specific case of lacking bonds is studied numerically and analytically.

PACS numbers: 87.16.Gj, 87.16.Dg, 61.72.Hh

The outer walls of biological cells are fluid bilayer membranes made by the self-assembly of lipid molecules in water [1]. For about three decades, the physical properties of these two-dimensional fluid surfaces, including elasticity, thermal fluctuations, phase behavior, topology, shape polymorphism, etc., have been thoroughly investigated in model systems [2, 3, 4]. In real cells, membranes host a large number of proteins and other inclusions, and they are attached to a network of filaments called the cytoskeleton [1]. In most cases this network is three-dimensional. In the case of red blood cells (RBC's), however, the cytoskeleton is a triangular two-dimensional network of flexible spectrin filaments attached to the membrane by proteins located at its vertices [5, 6, 7]. Recent experimental and theoretical studies have focused on the shape elasticity [8, 9, 10, 11, 12] and fluctuation properties [13, 14, 15, 16, 17] of these composite membranes. Up to now, the available theoretical models describing the RBC membrane fluctuations either are mean-field [15] or describe the cytoskeleton as a fixed plane producing a checkerboard (square) modulated potential [16]. In order to obtain a better description, it is essential to release the assumption of a fixed cytoskeletal plane and to allow for coupled fluctuations of the membrane and the cytoskeleton. It is also desirable to take into account the triangular nature of the cytoskeleton and to determine the effects of the cytoskeletal defects [17, 18].

In this paper, we propose a simple gaussian model describing the composite membrane of RBC's. It allows to calculate explicitely the whole fluctuation spectrum, even in the presence of cytoskeletal defects, such as lacking bonds and seven-fold or five-fold defects. We model the composite membrane (Fig. 1) as a triangular network of harmonic springs attached at its vertices to a fluid membrane described by a curvature Hamiltonian plus surface tension [19]. The only coupling between the two subsystems is the constraint that the cytoskeleton vertices lie within the membrane surface. As in model polymers [20], the gaussian character arises from neglecting the excluded volume between the

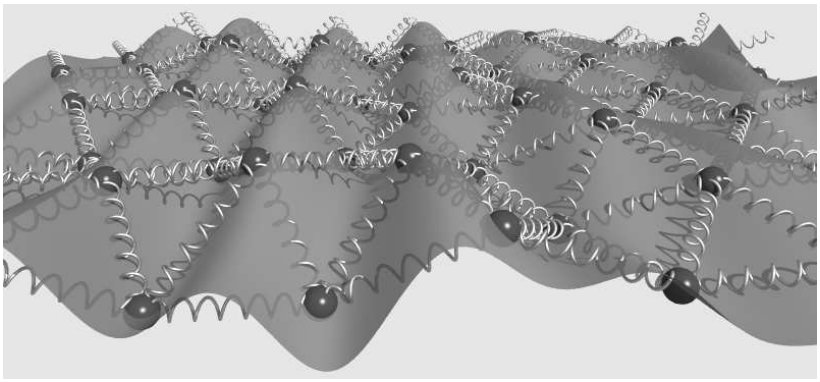

FIG. 1: Sketch of the model red blood cell (RBC) membrane.

*author for correspondance

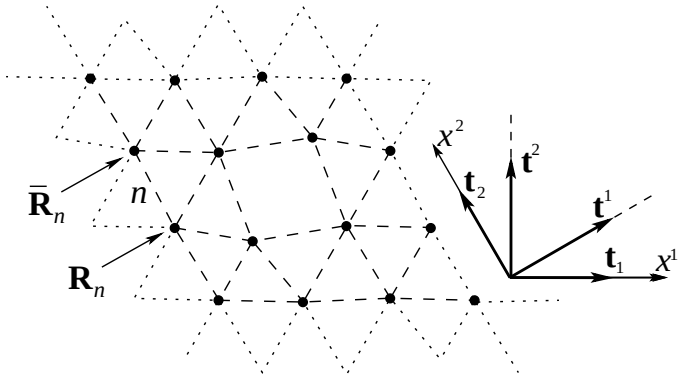

FIG. 2: Network of N springs (dashed lines) in a $M \times M$ unit cell of a cytoskeleton with periodic boundary conditions (dots) along the basis vectors $\mathbf{t}_1$ and $\mathbf{t}_2$. Here, $M = 3$ and $N = 26$. The extremities of the nth spring have projections $\mathbf{R}_n$ and $\overline{\mathbf{R}}_n$ onto the reference plane. A bond is lacking, in order to illustrate a simple situation with a density of defects.

membrane and the cytoskeleton (thereby treating the latter as "phantom" [21]). Depending on the experimental conditions, RBC fluctuations may be of thermal origin, or they may be driven by ATP consumption [22, 23]. Here, we consider only the thermal, equilibrium situation. We derive the height fluctuation spectrum $\langle |h_{\mathbf{q}}|^2 \rangle$ of our model system, and we discuss the crossover between the different regimes and the non-monotonic features arising from the membrane–cytoskeleton coupling. Since the cytoskeleton and its defects break the translational symmetry, we study the extinction conditions for the non-diagonal spectrum, i.e., $\langle h_{\mathbf{q}} h_{\mathbf{k}} \rangle$ for $\mathbf{k} \neq -\mathbf{q}$. We demonstrate that the latter reveals, in "dark field", the cytoskeletal defects. Detail studies should therefore allow to determine the nature and the density of the defects. Here, we discuss preliminary results concerning the spectral signature of lacking spectrin bonds.

Because of the triangular symmetry of the cytoskeleton, we introduce a planar reference frame with unitary basis vectors $\mathbf{t}_1$ and $\mathbf{t}_2$ making an angle of $2\pi/3$ (Fig. 2). We define the dual basis $(\mathbf{t}^1, \mathbf{t}^2)$ by $\mathbf{t}_\alpha \cdot \mathbf{t}^\beta = \delta_\alpha^\beta$, where δ_α^β is the Kronecker symbol. The metric tensor $g_{\alpha\beta} = \mathbf{t}_\alpha \cdot \mathbf{t}_\beta$ has diagonal (resp. off-diagonal) elements equal to 1 (resp. $-\frac{1}{2}$) and determinant $g = \det(g_{\alpha\beta}) = \frac{3}{4}$. Vectors in the plane will be represented by their coordinates according to $\mathbf{x} = x_\alpha \, \mathbf{t}^\alpha = x^\alpha \, \mathbf{t}_\alpha$ (Einstein summation assumed throughout), where $x^\alpha = g^{\alpha\beta} x_\beta$ with $g^{\alpha\beta} = g_{\alpha\beta}^{-1}$. We describe the membrane by its elevation $h(\mathbf{x}) \equiv h(x^\alpha)$ above a reference plane parallel to $(\mathbf{t}_1, \mathbf{t}_2)$ and we assume periodic boundary conditions such that $h(x^1, x^2) = h(x^1 + L_1, x^2) = h(x^1, x^2 + L_2)$, $\forall x^\alpha$. Our model Hamiltonian (per unit cell) is the following:

$$\mathcal{H} = \int_0^{L_1} \int_0^{L_2} \sqrt{g} \, dx^1 dx^2 \left[\frac{\kappa}{2} \left(\partial_\alpha \partial^\alpha h \right)^2 + \frac{\sigma}{2} (\partial^\alpha h)(\partial_\alpha h) \right] + \sum_{n=1}^{N} \frac{\mu_n}{2} \left[h(R_n^\alpha) - h(\bar{R}_n^\alpha) \right]^2 . \tag{1}$$

The first term, $\mathcal{H}_0[h]$, is the standard membrane Helfrich Hamiltonian [19] expressed in our non-orthonormal basis, with κ the membrane bending rigidity and σ an externally imposed surface tension. The second term, $\mathcal{V}[h]$, modeling the elasticity of the spectrin network, represents the stretching energy associated with the N springs that lie within the repeat period. In this expression, R_n^α and $\bar{R}_n^\alpha$ are the projections onto the reference plane of the extremities of the nth spring (Fig 2). We take for R_n^α and $\bar{R}_n^\alpha$ the equilibrium positions that they would occupy in the case the membrane were flat, since in the limit of small Gaussian fluctuations the in-plane and the out-of-plane fluctuations of the vertices are decoupled. We allow for any kind of defect or heterogeneity, therefore we do not assume that R_n^α and $\bar{R}_n^\alpha$ make a regular triangular network. The constant μ_n is related to the rigidity k and free-length ℓ of the springs (which we assume to be identical biological elements) and to the geometry in the following way: to second order in h, the spring elongation energy $\frac{1}{2} k [\{(\mathbf{R}_n - \overline{\mathbf{R}}_n)^2 + [h(\mathbf{R}_n) - h(\overline{\mathbf{R}}_n)]^2\}^{1/2} - \ell]^2$ gives the in-plane contribution $\frac{1}{2} k (|\mathbf{R}_n - \overline{\mathbf{R}}_n| - \ell)^2$ plus the term $\mathcal{V}[h]$ of Eq. (1), with

$$\mu_n = k \left(1 - \ell |\mathbf{R}_n - \overline{\mathbf{R}}_n|^{-1} \right) . \tag{2}$$

Because the network may have been stretched or compressed, either mechanically or osmotically, or because of the possible defects, the μ_n may have either sign.

Let us define a Fourier transform by $h(x^1, x^2) = (\sqrt{g} L_1 L_2)^{-1/2} \sum_{\mathbf{q}} h_{\mathbf{q}} \, e^{i q_\alpha x^\alpha}$ where the wavevectors are quantified as $q_\alpha = n_\alpha 2\pi / L_\alpha$, where $n_\alpha \in \mathbb{Z}$. In order to work with dimensionless quantities, we normalize the energies by $k_{\mathrm{B}} T \equiv \beta^{-1}$, the in-plane lengths by $\xi_\sigma = \sqrt{\kappa/\sigma}$ and the membrane height $h(x^\alpha)$ by $1/\sqrt{\beta\sigma}$. Hence $h_{\mathbf{q}}$ is normalized

by $\sqrt{\kappa/\beta}\,\sigma^{-1}$ and μ_n by σ. Unless otherwise specified, all quantities are now dimensionless. We thus have $\mathcal{H}_0 = \sum_{\mathbf{q},\mathbf{k}} \frac{1}{2} h_{\mathbf{q}} G^{-1}_{\mathbf{q},\mathbf{k}} h_{\mathbf{k}}$ where $G_{\mathbf{q},\mathbf{k}} = \delta_{\mathbf{q}+\mathbf{k}}/(\mathbf{q}^2+\mathbf{q}^4)$ and $\mathbf{q}^2 = q^\alpha q_\alpha$, yielding the correlation function of the bare membrane:

$$G(\mathbf{x}) = \langle h(\mathbf{0}) h(\mathbf{x}) \rangle = \frac{1}{\sqrt{g} L_1 L_2} \sum_{\mathbf{q}} \frac{e^{i q_\alpha x^\alpha}}{\mathbf{q}^2 + \mathbf{q}^4} \,. \tag{3}$$

For an infinite membrane, this gives a Bessel function of the second kind: $G(\mathbf{x}) = -\frac{1}{4} \mathrm{Y}_0(|\mathbf{x}|)$. Because $\mathcal{H}$ is not diagonal in $\mathbf{q}$-space due to the dependence in $\mathbf{R}_n$ and $\overline{\mathbf{R}}_n$, it cannot be directly inverted to yield the full correlation function $G(\mathbf{x}) = \langle h(\mathbf{0}) h(\mathbf{x}) \rangle$. To proceed, we add an external field, $\mathcal{H} \to \mathcal{H} + \sum_{\mathbf{q}} h_{\mathbf{q}} f_{-\mathbf{q}}$, and we calculate $\langle h_{\mathbf{q}} h_{\mathbf{k}} \rangle = -\partial^2 F / (\partial f_{-\mathbf{q}} \partial f_{-\mathbf{k}})|_{f=0}$, where $F = -\ln[\int \mathcal{D}[h] \exp(-\mathcal{H})]$ is the free-energy. In order to integrate the membrane degrees of freedom, we rewrite $\exp(-\mathcal{V})$ with the help of auxialiary fields (one for each spring) as

$$\int \prod_n d\phi_n \, \exp \sum_n \left(-\frac{\phi_n^2}{2\mu_n} + i \phi_n [h(R_n^\alpha) - h(\bar{R}_n^\alpha)] \right). \tag{4}$$

Sums and products over n (and further on m) implicitely run from 1 to N. Performing the gaussian integral over h yields $\exp(-F) = \int \prod_n d\phi_n \, \exp(-\tilde{\mathcal{H}})$, where

$$\tilde{\mathcal{H}} = \sum_n \frac{\phi_n^2}{2\mu_n} - \frac{1}{2} \sum_{\mathbf{q},\mathbf{k}} (S_{-\mathbf{q}} - f_{-\mathbf{q}}) \, G_{\mathbf{q},\mathbf{k}} \, (S_{-\mathbf{k}} - f_{-\mathbf{k}}) \,, \tag{5}$$

in which $S_{\mathbf{q}} = (\sqrt{g} L_1 L_2)^{-\frac{1}{2}} \sum_n i \phi_n (e^{-i q_\alpha R_n^\alpha} - e^{-i q_\alpha \bar{R}_n^\alpha})$. The integral over the ϕ_n is again Gaussian, yielding $F[f] = -\frac{1}{2} \sum_{\mathbf{q},\mathbf{k}} f_{-\mathbf{q}} G_{\mathbf{q},\mathbf{k}} f_{-\mathbf{k}} + \delta F[f]$, with

$$\delta F[f] \,=\, \frac{1}{2} \sum_{n,m} \left(\sum_{\mathbf{q}} c_{\mathbf{q}}^{(n)} f_{-\mathbf{q}} \right) B^{-1}_{nm} \left(\sum_{\mathbf{k}} c_{\mathbf{k}}^{(n)} f_{-\mathbf{k}} \right), \tag{6}$$

where

$$c_{\mathbf{q}}^{(n)} \;=\; \frac{1}{(\sqrt{g} L_1 L_2)^{\frac{1}{2}}} \frac{e^{-i q_\alpha R_n^\alpha} - e^{-i q_\alpha \bar{R}_n^\alpha}}{\mathbf{q}^2 + \mathbf{q}^4} \,, \tag{7}$$

$$B_{nm} \;=\; \frac{1}{\mu_n} \delta_{nm} + G(\mathbf{R}_n - \mathbf{R}_m) - G(\mathbf{R}_n - \overline{\mathbf{R}}_m) - G(\overline{\mathbf{R}}_n - \mathbf{R}_m) + G(\overline{\mathbf{R}}_n - \overline{\mathbf{R}}_m) \,. \tag{8}$$

It follows that the full correlation function $\Gamma_{\mathbf{q},\mathbf{k}} = \langle h_{\mathbf{q}} h_{\mathbf{k}} \rangle = G_{\mathbf{q},\mathbf{k}} + \Delta\Gamma_{\mathbf{q},\mathbf{k}}$ is given, with no approximation, by

$$\Gamma_{\mathbf{q},\mathbf{k}} = \frac{\delta_{\mathbf{q}+\mathbf{k}}}{\mathbf{q}^2 + \mathbf{q}^4} - \sum_{n,m=1}^{N} c_{\mathbf{q}}^{(n)} \, B^{-1}_{nm} \, c_{\mathbf{k}}^{(m)}. \tag{9}$$

For weak cytoskeletal strains, i.e., $\mu_n = \mathcal{O}(\mu) \ll 1$, we have $B^{-1}_{nm} = \mu_n \delta_{nm} + \mathcal{O}(\mu^2)$, and thus

$$\Delta\Gamma_{\mathbf{q},\mathbf{k}} \simeq -\frac{1}{\sqrt{g} L_1 L_2} \sum_{n=1}^{N} \mu_n \frac{\psi_{n,\mathbf{q}} \, \psi_{n,\mathbf{k}}}{(\mathbf{q}^2 + \mathbf{q}^4)(\mathbf{k}^2 + \mathbf{k}^4)} \tag{10}$$

where $\psi_{n,\mathbf{q}} = e^{-i \mathbf{q} \cdot \mathbf{R}_n} - e^{-i \mathbf{q} \cdot \overline{\mathbf{R}}_n}$. The fluctuation spectrum can thus be obtained analytically for weak strains even in presence of defects, or, for larger strains, numerically by simply inverting a $N \times N$ matrix.

Uniform cytoskeleton. – In the case of a uniform dilation or compression in the absence of defects, the points $\mathbf{R}_n$ and $\overline{\mathbf{R}}_n$ form a regular triangular lattice with $\mu_n = \mu$, $\forall n$, corresponding to a uniform meshsize ξ such that $N = 3 L_1 L_2 / \xi^2$. Thus, in dimensional units and for small values of μ/σ, Eq. (10) gives for $\mathbf{k} = -\mathbf{q}$ the following fluctuation spectrum:

$$\langle |h_{\mathbf{q}}|^2 \rangle \simeq \frac{k_{\mathrm{B}} T}{\sigma \, \mathbf{q}^2 + \kappa \, \mathbf{q}^4} - \frac{4 \mu \, g^{-\frac{1}{2}} \xi^{-2} \, k_{\mathrm{B}} T}{(\sigma \, \mathbf{q}^2 + \kappa \, \mathbf{q}^4)^2} \sum_{j=0}^{2} \sin^2 \left[\frac{q\xi}{2} \cos(\theta - \frac{j\pi}{3}) \right], \tag{11}$$

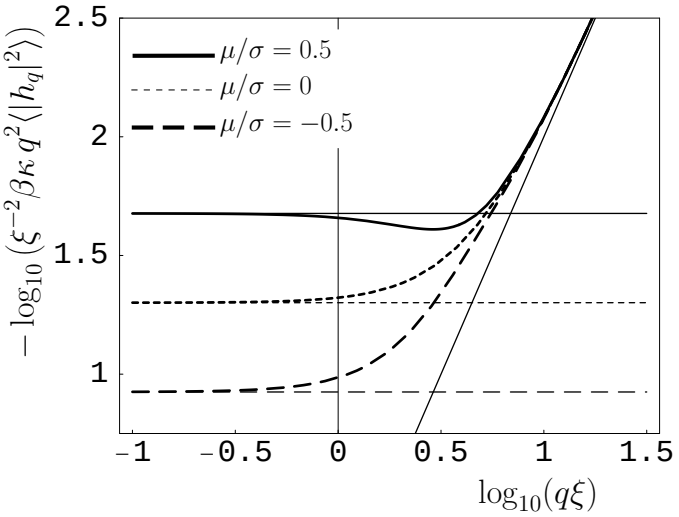

FIG. 3: Fluctuation spectrum of the model RBC membrane with a uniform triangular cytoskeleton, for a tension corresponding to $\sqrt{\sigma/\kappa} \simeq 4.5\,\xi^{-1}$ and a direction of $\mathbf{q}$ corresponding to $\theta = 0$. The case $\mu > 0$ (resp. $\mu < 0$) corresponds to a stretched (resp. compressed) cytoskeleton. We chose $|\mu|/\sigma = 0.5$ to better emphasize the features of the curves, although Eq. (11) is valid in the limit $\mu \ll \sigma$. All quantities are in dimensional units.

with θ the angle between $\mathbf{t}_1$ and $\mathbf{q}$. For $q \ll \xi^{-1}$, we get $k_{\rm B}T/\langle|h_{\mathbf{q}}|^2\rangle \simeq \sigma_{\rm eff}\, q^2 + \kappa_{\rm eff}\, q^4$, with

$$\sigma_{\rm eff} \;\simeq\; \sigma + \frac{3}{2\sqrt{g}}\,\mu \;=\; \sigma + \frac{k}{\sqrt{3}}\,(1-\ell/\xi), \tag{12}$$

$$\kappa_{\rm eff} \;\simeq\; \kappa - \frac{3}{32\sqrt{g}}\,\mu\xi^2 \;=\; \kappa + \frac{\sqrt{3}}{16}\,k\xi\,(\xi-\ell)\;, \tag{13}$$

and for $q \gg \xi^{-1}$, Eq. (11) yields the bare membrane spectrum $k_{\rm B}T/\langle|h_{\mathbf{q}}|^2\rangle \simeq \sigma\, q^2 + \kappa\, q^4$. We thus recover the effective tension jump $\sigma - \sigma_{\rm eff}$ discussed in Refs. [14, 15]. In addition, we obtain the renormalization of the bending rigidity $\kappa_{\rm eff}$ due to the cytoskeleton. Taking $k \simeq 10^{-5}$ J/m^2 [12] and $\xi \approx \ell \simeq 10^{-7}$ m [24], we obtain $\kappa_{\rm eff} - \kappa \simeq 10^{-20}$ J, wich is comparable but smaller than the usual membrane bending rigidity, in agreement with the measurements of Ref. [25].

The full fluctuation spectrum for large tensions, i.e., $\sigma > \kappa/\xi^2$, is shown in Fig. 3. There are three regimes: i) a flat, tension-dominated regime for $q < \xi^{-1}$, revealing $\sigma_{\rm eff}$, ii) a crossover region $\xi^{-1} < q < \sqrt{\sigma/\kappa}$, showing the transition from $\sigma_{\rm eff}$ to σ and thus exhibiting a negative slope for large enough $\mu > 0$, iii) a terminal linear regime dominated by the bending rigidity, revealing κ. In the case of weak tensions, i.e., $\sigma < \kappa/\xi^2$ (not shown), the transition to the terminal regime occurs before q reaches ξ^{-1}, hence the change in tension becomes invisible. Since $\kappa_{\rm eff} \simeq \kappa$, one does not see either the slope change occuring around $q \simeq \xi^{-1}$. The curves thus look like the dashed ones in Fig. 3, except that the intersection of the asymptotes occurs in the region $q < \xi^{-1}$.

Cytoskeleton with defects. – Let us discuss the general conditions under which the couplings $\langle h_{\mathbf{q}} h_{\mathbf{k}}\rangle$ are extinct or not. Our Hamiltonian can be expressed as $\mathcal{H} = \int d^2x\, d^2r\, h(\mathbf{x})\, H(\mathbf{x},\mathbf{r})\, h(\mathbf{x}+\mathbf{r}) = \int d^2q\, d^2k\, h_{\mathbf{q}}\, \bar{H}_{\mathbf{q},\mathbf{k}}\, h_{\mathbf{k}}$. In the absence of a cytoskeleton, the translational invariance of the system yields the well-known non-extinction condition $\mathbf{q} = -\mathbf{k}$. In the presence of a cytoskeleton, this invariance breaks down. For a perfectly uniform cytoskeleton, however, $H(\mathbf{x},\mathbf{r})$ remains invariant for discrete translations of the form $x^\alpha \to x^\alpha + \xi$ and the non-extinction condition becomes $q_\alpha = -k_\alpha$ *modulo* $2\pi/\xi$. This weaker condition is still strong, because $2\pi/\xi$ is very large (macroscopically). Now, in the presence of random structural defects, the translational symmetry vanishes and all the couplings $\langle h_{\mathbf{q}} h_{\mathbf{k}}\rangle$ appear [26].

There are mainly two types of defects: lacking bonds and dislocations made by pairs of five-fold and seven-fold defects [17, 18]. A systematic study of the signature of these defects according to their density and type is outside the scope of this paper [27]. Here, we limit ourselves to the simplest situation, i.e., lacking bonds, as in Fig. 2. We show in Fig. 4 the corresponding non-diagonal spectrum (i.e., $\langle h_{\mathbf{q}} h_{\mathbf{k}}\rangle$ with $\mathbf{q} \neq -\mathbf{k}$) for $\mathbf{q} = q\,\mathbf{t}^1/\|\mathbf{t}^1\|$ and $\mathbf{k} = -q\,\mathbf{t}^2/\|\mathbf{t}^2\|$, as obtained from Eq. (10) after numerically minimizing the in-plane elastic energy in order to determine the positions R_n^α and $\bar{R}_n^\alpha$ of the springs ends. A satisfying analytical approximation of this spectrum (Fig. 4) can be obtained by neglecting the lattice distorsion, i.e., by using the positions R_n^α and $\bar{R}_n^\alpha$ of the regular lattice while setting one of the μ_n to zero. In this case, Eq. (10) gives $|\langle h_{\mathbf{q}} h_{\mathbf{k}}\rangle| = \mu\, k_{\rm B}T g^{-\frac{1}{2}} L^{-2} |\sin(\mathbf{q}\cdot\mathbf{r})\sin(\mathbf{k}\cdot\mathbf{r})|(\sigma q^2 + \kappa q^4)^{-2}$, with $\mathbf{r} = \frac{1}{2}\xi\mathbf{u}$

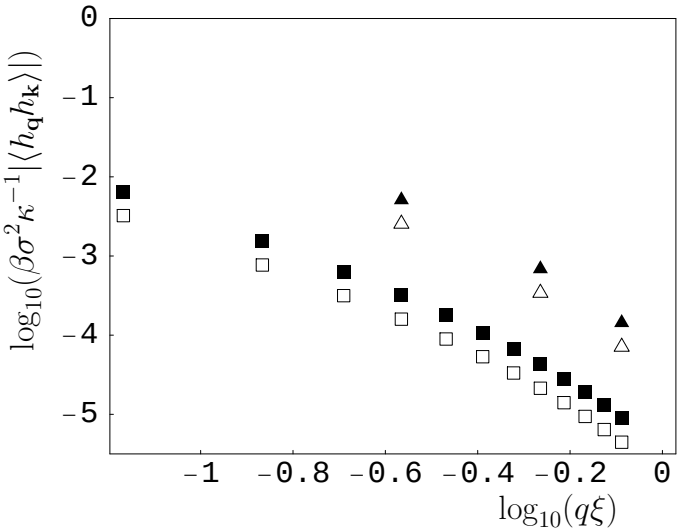

FIG. 4: Non-diagonal fluctuation spectrum $\langle h_{\mathbf{q}}h_{\mathbf{k}}\rangle$ in the presence of lacking bonds, for $\mathbf{q} \neq -\mathbf{k}$ but $\|\mathbf{q}\| = \|\mathbf{k}\| = q$, as detailed in the text. The squares (resp. triangles) correspond to one missing bond per unit cell, as in Fig. 2, but for $M = 80$ (resp. $M = 20$). The values of q are quantified by the periodic boundary conditions. The filled symbols are numerically calculated from Eq. (10), while the open symbols correspond to the analytical approximation discussed in the text.

where $\mathbf{u}$ is the unit vector parallel to the missing bond. In the $q \to 0$ limit, we obtain

$$|\langle h_{\mathbf{q}}h_{\mathbf{k}}\rangle| \approx \frac{\mu\, k_{\mathrm{B}}T}{\sigma^2 q^2}\,\rho\,, \tag{14}$$

which shows that the non-diagonal spectrum is proportional to the defect density $\rho = 1/(3M^2)$.

In conclusion, in the light of this model experimental measurements of RBC equilibrium fluctuations under strain could give new informations concerning the structure and elasticity of the cytoskeleton. Since the defects and the plasticity of RBC's are believed to be controled by the ATPase activity [17], it should also be interesting to investigate the (equilibrium) non-diagonal spectrum at various stages of the erythrocyte life or in particular conditions, such as capillary transport. Finally, it should be possible to study in a Langevin picture the dynamical properties of this model system, thereby determining the consequence of non-equilibrium ATP-driven noise on the fluctuation spectrum. This would be extremely interesting, as recent experiments reveal strong non-equilibrium effects [17, 22, 23].

Acknowledgments

We thank Dr. David Lacoste for stimulating discussions at the early stage of this work and Prof. Ken Sekimoto for precious comments and fuitfull discussions all along.

[1] B. Alberts, A. Johnson, J. Lewis, M. Raff, K. Roberts, P. Walter, *Molecular Biology of the Cell* (Garland, New York, 2002), 4th ed.
[2] *Statistical Mechanics of Membranes and Interfaces*, D. R. Nelson, T. Piran, S. Weinberg eds. (World Scientific, Singapore, 1989).
[3] S. A. Safran, *Statistical Thermodynamics of Surfaces, Interfaces, and Membranes* (Addison-Wesley Publishing Company, 1994).
[4] O. G. Mouritsen, *Life—as a matter of fat* (The frontiers collection, Springer, Berlin, 2005).
[5] T. J. Byers and D. Branton, *Proc. Natl. Acad. Sci. USA* **82**, 6153 (1985).
[6] V. Bennett, *Biochim. Biophys. Acta* **988**, 107 (1989).
[7] N. Mohandas and E. Evans, *Annu. Rev. Biophys. Biomol. Struct.* **23**, 787 (1994).
[8] S. K. Boey, D. H. Boal, and D. E. Discher, *Biophys. J.* **75**, 1573 (1998), *Biophys. J.* **75**, 1584 (1998).
[9] D. H. Boal, *Biol. Bull.* **194**, 331 (1998).
[10] G. H. W. Lim, M. Wortis and R. Mukhopadhyay, *PNAS* **99**, 16766 (2002).

[11] R. Mukhopadhyay, G. H. W. Lim and M. Wortis, *Biophys. J.* **82**, 1756 (2002).
[12] G. Lenormand, S. Henon, A. Richert, J. Simeon and F. Gallet, *Biophys. J.* **81**, 43 (2001).
[13] A. Zilker, H. Engelhardt and E. Sackmann, *J. Physique* **48**, 2139 (1987).
[14] N. Gov, A. G. Zilman, and S. A. Safran, *Phys. Rev. Lett.* **90**, 228101 (2003).
[15] J.-B. Fournier, D. Lacoste and E. Raphaël, *Phys. Rev. Lett.* **92**, 018102 (2004).
[16] N. Gov and S. A. Safran, *Phys. Rev. E* **69**, 011101 (2004).
[17] N. Gov and S. A. Safran, *Biophys. J.* **88**, 1859 (2005).
[18] H. S. Seung and D. R. Nelson, *Phys. Rev. A* **38**, 1005 (1988).
[19] W. Helfrich, *Z. Naturforsch.* C **28**, 693 (1973).
[20] P.-G. de Gennes, *Scaling concepts in polymer physics* (Cornell University Press, London, 1986).
[21] Y. Kantor and D. R. Nelson, *Phys. Rev. Lett.* **58**, 2774 (1987).
[22] S. Tuvia et al., *PNAS* **94**, 5045 (1997).
[23] S. Tuvia, S. Levin, A. Bitler, and R. Korenstein, *J. Cell. Biol.* **141**, 1551 (1998).
[24] B. W. Shen, R. Josephs, and T. L. Steck, *J. Cell. Biol.* **102**, 997 (1986).
[25] H. Strey, M. Peterson, and E. Sackmann, *Biophys. J* **69**, 478 (1995).
[26] For an array of defects, however, there will be (weak) extinction conditions due to the translational symmetry.
[27] C. Dubus and J.-B. Fournier, in preparation.